Performance Comparison of Sliding Mode and Instantaneous Reactive Power Theory Control Techniques for Three-Phase Active Power Filter

Eric Nwokolo[1], Ifeanyi Chinaeke-Ogbuka[2], Augustine Ajibo[2], Cosmas Ogbuka[1,3,4], Uche Ogbuefi[1,3], and Emenike Ejiogu[1,3,4]
[1]Department of Electrical Engineering, University of Nigeria Nsukka, Nigeria
[2]Department of Electronic Engineering, University of Nigeria Nsukka, Nigeria
[3]Africa Centre of Excellence for Sustainable Power and Energy Development, University of Nigeria Nsukka, Nigeria
[4]Laboratory of Industrial Electronics, Power Devices and New Energy Systems, University of Nigeria Nsukka, Nigeria
Email: nwokoloeric@yahoo.com; {ifeanyi.chinaeke-ogbuka; augustine.ajibo; cosmas.ogbuka; uche.ogbuefi; emenike.ejiogu}@unn.edu.ng

Abstract—**The performance comparison of Sliding Mode (SM) control and instantaneous reactive power theory (PQ) control for three-phase Active Power Filter (APF) is presented. Algorithms for SM and PQ techniques were developed and used in the control of APF to shunt harmonics due to non-linear loads from the power grid. Total Harmonic Distortion (THD) was used for performance verification. The PQ control reduced the THD value, on average, from 29.84% to 4.937% while the SM control reduced the THD value, on average, from 29.84% to 5.27%. The results obtained show that PQ control offered slightly better performance in terms of reduced THD than the SM control even though the implementation of SM was less complex due to the use of programmable chips. In addition, the SM control recovered faster from transient disturbances than the PQ algorithm. Both results are, however, within the conformity limit of the IEEE standard and have proven to be good for harmonic mitigation. MATLAB/Simulink 2018 version was used as the simulation tool.**

Index Terms—**Sliding-mode, instantaneous reactive power, active power filter, harmonics mitigation, total harmonic distortion**

I. Introduction

Harmonic distortions are of significant concern in power quality research [1]-[9]. Harmonics in grid power supplies have been a topic of great interest and the use of active power filters for harmonic mitigation have been reported in the literature.

Current harmonics control using active power filters (APFs) and filters comparison were presented in [10] with the circuits capable of complexity reduction. A 3-level inverter topology characterized using Bidirectional Neutral Point Clamped (BNPC) inverter involving energy-based Lyapunov control was presented in [11] for harmonic compensation of loads. APFs circuit configuration which used a neural network controller having fast speed of response on a 3-phase voltage source active power filters connected in shunt configuration and referred to as shunt active power filter (SAPF) was presented in [12]-[14] while the work in [15] shows the use of phase-shift technique in harmonic detection. Other circuit configurations for harmonic compensation such as hybrid APF [16]-[17], use of fuzzy logic for Cascaded H-Bridge Multi-Level Inverter [18], type-2 fuzzy logic controlled three-level shunt active power filter [19], multilevel inverters for selective harmonic elimination [20], [21]

Analysis of novel harmonic filtering strategy that uses phase-shifting; mitigation of power quality problems based on discrete time filtering (Wiener filtering) for reference supply and distorted current extraction and the use of extended Kalman Filter (KF) for system state-space variable estimation incorporated in a sliding mode controller were presented in [22]-[25]. Optimal control of shunt active power filter to meet IEEE std. 519 current harmonic constraints under non-ideal supply condition was presented in [26] while [27] presented a verifications based on 3-phase PWM voltage converter connected to AC mains. An optimal control algorithm for power factor improvement on the converter topology was presented in [28]. The power quality issue of harmonics using capacitor-clamped voltage source inverter [29], neural APF [30] and sliding mode control technique [31]-[33] presented different trending control methods. A clear gap exists in comparing different methods of harmonic mitigation.

In the present work, a comparison of the performance of sliding model-based control and instantaneous reactive power (PQ) theory on harmonic mitigation using three-phase Shunt Active Power Filters (SAPF) for industrial application is presented. The major interest is on harmonic mitigation of the odd harmonics using three-phase SAPF coupled with capacitor dc bank with the aid of a passive circuit. Detailed development of mathematical algorithms for the two methods was done in section II. Simulations and discussion of results were done in section III while section IV was devoted to conclusion of the work.

Manuscript received June 8, 2020; revised September 4, 2020; accepted October 4, 2020.

Corresponding author: Cosmas Uchenna Ogbuka (email: cosmas.ogbuka@unn.edu.ng).

doi: 10.18178/ijeetc.10.2.83-90

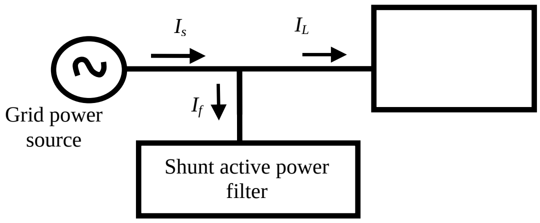

Fig. 1. Principle of compensation action of SAPF.

II. Development of Mathematical Algorithm

Mathematical Algorithm based on SM control, PQ theory control and stability test of the sliding mode were presented. Considering the single line diagram shown in Fig. 1.

$$p_{\text{tload}}(t) = p_{\text{fload}}(t) + q_{\text{rload}}(t) + p_{\text{hload}}(t) \tag{1}$$

with $p_{\text{fload}}(t)$, $q_{\text{rload}}(t)$ and $p_{\text{hload}}(t)$ being the instantaneous real, reactive and harmonic powers respectively drawn by the load and $p_{\text{fload}}(t)$ obtained by the difference of the real power by the AC mains, $p_{\text{ac-source}}(t)$ and the real component of power from the utility contributing to $p_{\text{ac-loss}}$ which accounts for the switching losses of the supply and to ensure a constant dc link voltage.

Assuming the source reactive power $q_{\text{ac-source}}(t)$ to be zero, the real power drawn by the load is obtained by adding the real and harmonic powers drawn by the load while the reactive power drawn by the load is obtained by adding the reactive and harmonic powers drawn by the load. Also, the real power supplied by the APF is obtained by subtracting the real ac power loss from the real power drawn by the load while the reactive power supplied by APF is summation of reactive power and harmonic power drawn by the load.

A. Estimation of Reference Source Current

From Fig. 1, applying Kirchhoff's current law and considering industrial loads, which are usually nonlinear in nature, the load current $i_{\text{load}}(t)$ has two components: the fundamental component $i_{\text{load}_0}(t)$ and the harmonic components $i_{\text{load}_h}(t)$ as in (2)

$$i_s(t) = i_{\text{load}_0} \sin(\omega t + \theta_0) + \sum_{k=2}^{\infty} i_{\text{load}_{hk}} \sin(k\omega t + \theta_k) + i_{\text{filter}}(t) \tag{2}$$

Also,

$$u_s(t) = u_m \sin \omega t \tag{3}$$

where $i_s(t)$, $i_{\text{load}}(t)$, $i_{\text{filter}}(t)$, $u_s(t)$, u_m , i_{load_0} , θ_0 , $i_{\text{load}_{hk}}$, and θ_k represent the instantaneous value of source current, load current, filter current, instantaneous and peak values of the source voltage, the amplitude of the fundamental load currents, angle deviation from fundamental voltage, kth harmonic load current, and kth angle of deviation from voltage.

However, the total instantaneous load power expressed as $p_{\text{tload}}(t)$ can be stated as:

$$p_{t_{\text{load}}}(t) = u_s(t) i_{\text{load}}(t) \tag{4}$$

Substituting the first two components of (2) which constitute $i_{\text{load}}(t)$ and (3) into (4) and applying trigonometric identities to the result gives:

$$\begin{aligned} p_{\text{tload}}(t) = {} & u_m i_{\text{load}_0} (\sin \omega t)^2 \cos \theta_0 + \\ & u_m i_{\text{load}_0} \sin \omega t \cos \omega t \sin \theta_0 + \\ & u_m \sin \omega t \sum_{k=2}^{\infty} i_{\text{load}_{hk}} \sin(k\omega t + \theta_k) \end{aligned} \tag{5}$$

By comparing (5) with the equation usually given by $p_{\text{fload}}(t)$, it can be deduced as

$$p_{\text{fload}}(t) = u_m i_{\text{load}_0} (\sin \omega t)^2 \cos \theta_0 \tag{6}$$

In compensation, it is typical that the real power $p_{\text{fload}}(t)$ is supplied by the source. All other components $q_{\text{rload}}(t)$ and $p_{\text{hload}}(t)$ are supplied by the SAPF. Therefore,

$$p_{\text{filter}}(t) = q_{\text{rload}}(t) + p_{\text{hload}}(t) \tag{7}$$

Substituting (6) into the source power form of (4) and making $i_s(t)$ the subject gives:

$$i_s(t) = i_{\text{load}_o} \cos \theta_0 \sin \omega t \tag{8}$$

The total source current is an addition of (8) and the total loss component of current taken from the source for switching operation, $i_{\text{sw-loss}}$. This accounts for the switching losses in the inverter circuit.

From the foregoing, to design SAPF that compensate for reactive and harmonic power, the inverter circuit must be guided by the (9):

$$i_{\text{filter}}(t) = i_s(t) - i_{\text{load}}(t) \tag{9}$$

B. Mode of Switching of the APF Circuit

Fig. 2 shows the power circuit of the APF. Switching action takes place in pairs. That is one switch ON, the other OFF as follows (p_1, p_4), (p_3, p_6), and (p_5 p_2) at a time. The six distinct switching states are shown as: State One (p_1, p_6, p_5), State Two (p_1, p_6, p_2), State Three (p_1, p_3, p_2), State Four (p_4, p_3, p_2), State Five (p_4, p_3, p_5), State Six (p_4, p_6, p_5). This switching sequence produces the output voltages and current. With this scheme, the instantaneous voltages of the active filter are $u_{\text{af}}, u_{\text{bf}}, u_{\text{cf}}$ and $+u_{\text{dc}}$ or zero. Also, line-to-line output voltages $u_{\text{ab}}, u_{\text{bc}}$,and u_{ca} are $+u_{\text{dc}}$, zero or $-u_{\text{dc}}$.

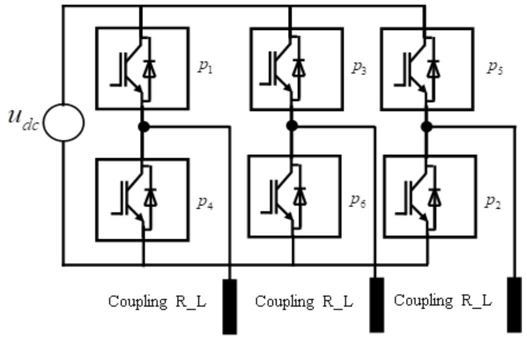

Fig. 2. APF Power circuit with coupling filter.

The switching function, t_m of the mth leg(abc) of the APF as: t_k which is either 1 or 0 and its prime being a complement of the initial digital state. Since the APF voltage u_{mf} per phase is dependent on the switching state t_k, where $k = 1, 2, \cdots, 6$. Thus:

$$u_{\text{mf}} = t_m u_{\text{dc}} \tag{10}$$

By applying Kirchhoff's rules for voltages and currents at the point of common contact, PCC (output side of the active power circuit with a coupling filter per phase) and with the switching state (t_m) converted to switching function (d_m) and considering absence of zero sequence in AC currents, the complete model of the APF in the "abc" referential is obtained as shown in (11)

$$\begin{aligned}\frac{d}{dt}\begin{bmatrix} i_{\text{fa}} \\ i_{\text{fb}} \\ u_{\text{dc}} \end{bmatrix} &= \begin{bmatrix} -r_{\text{fa}}/l_{\text{fa}} & 0 & 0 \\ 0 & -r_{\text{fb}}/l_{\text{fb}} & 0 \\ 0 & 0 & 0 \end{bmatrix}\begin{bmatrix} i_{\text{fa}} \\ i_{\text{fb}} \\ u_{\text{dc}} \end{bmatrix} + \\ &\begin{bmatrix} -u_{\text{dc}}/l_{\text{fa}} & 0 & 0 \\ 0 & -u_{\text{dc}}/l_{\text{fa}} & 0 \\ i_{\text{fa}}/c_f & i_{\text{fb}}/c_f & 0 \end{bmatrix}\begin{bmatrix} d_a \\ d_b \\ 0 \end{bmatrix} + \\ &\begin{bmatrix} 1/l_{\text{fa}} & 0 & 0 \\ 0 & 1/l_{\text{fb}} & 0 \\ 0 & 0 & 0 \end{bmatrix}\begin{bmatrix} u_{\text{sa}} \\ u_{\text{sb}} \\ 0 \end{bmatrix}\end{aligned} \tag{11}$$

In other to equalize the instantaneous power flow on the DC-AC side of the APF considering only fundamental component, it implies that from Fig. 2

$$\begin{aligned} u_{\text{dc}} i_{\text{dc}} = u_{sa} i_{sa} & \sin\omega t \sin(\omega t - \varphi_a) + \\ & u_{\text{sb}} i_{\text{sb}} \sin(\omega t - \frac{2\pi}{3}) \sin(\omega t - \frac{2\pi}{3} - \varphi_b) + \\ & u_{\text{sc}} i_{\text{sc}} \sin(\omega t + \frac{2\pi}{3}) \sin(\omega t + \frac{2\pi}{3} - \varphi_c) \end{aligned} \tag{12}$$

Applying equation d-q transformation on the dynamic model of the APF in the d-q frame gives:

$$\begin{aligned}\frac{d}{dt}\begin{bmatrix} i_{\text{fd}} \\ i_{\text{fq}} \\ u_{\text{dc}} \end{bmatrix} &= \begin{bmatrix} -r_{\text{fa}}/l_{\text{fa}} & \omega & 0 \\ -\omega & -r_{\text{fb}}/l_{\text{fb}} & 0 \\ 0 & 0 & 0 \end{bmatrix}\begin{bmatrix} i_{\text{fd}} \\ i_{\text{fq}} \\ u_{\text{dc}} \end{bmatrix} + \\ &\begin{bmatrix} -u_{\text{dc}}/L_{\text{fx}} & 0 & 0 \\ 0 & -u_{\text{dc}}/L_{\text{fy}} & 0 \\ i_{\text{fd}}/c_f & i_{\text{fq}}/c_f & 0 \end{bmatrix}\begin{bmatrix} d_d \\ d_q \\ 0 \end{bmatrix} + \\ &\begin{bmatrix} 1/l_{\text{fa}} & 0 & 0 \\ 0 & 1/l_{\text{fb}} & 0 \\ 0 & 0 & 0 \end{bmatrix}\begin{bmatrix} u_{\text{sd}} \\ u_{\text{sq}} \\ 0 \end{bmatrix}\end{aligned} \tag{13}$$

C. Mode of Switching of the APF Circuit

Generally, the sliding surface is chosen to be a linear combination of state variables. Here, the three state variables $[i_{fd} \quad i_{fq} \quad u_{dc}] = [x_1 \quad x_2 \quad x_3]$ which involve two inductors current and the other involving the dc output voltage. Two currents had to track their respective harmonic references. In addition, the DC voltage must be regulated at a fixed set point. Thus, the sliding surface s_s is defined as

$$s_s(x) = c_i x_0 + c_v x_v \tag{14}$$

where c_i and c_v are the sliding surface coefficients which must be carefully chosen to ensure that the sliding mode exists at minimum around the desired equilibrium point. On reaching the surface, the dynamics of the system lead toward the equilibrium point.

More so, x_0 and x_v are the state variables defined as $x_0 = x_i - x_{\text{load}}^*$ and $x_v = u_{\text{dc}} - u_{\text{dc}}^*$ respectively, where, x_{load}^* is the corresponding nonlinear load currents that is transformed to the synchronous reference frame, u_{dc} is the component of the APF and u_{dc}^* is the reference voltage of the system.

Applying (14) as in this case, the sliding mode switching functions were given as

$$s_{\text{si}}(x) = \begin{bmatrix} s_{\text{sd}} \\ s_{\text{sq}} \end{bmatrix} = \begin{bmatrix} c_i(x_1 - x_1^*) + c_v(x_3 - x_3^*) \\ c_i(x_2 - x_2^*) \end{bmatrix} \tag{15}$$

The two-sliding mode switching functions are linear. These are to control the legs a, b, and c using the two switching functions s_{sd} and s_{sq}.

There were many approaches to this, using the form shown in (16)

$$u_i = u_{\text{ieq}} + u_{\text{iN}} \tag{16}$$

Thus,

$$\begin{aligned} \dot{S}_{\text{si}} &= Q(\dot{x} - \dot{x}_{\text{load}}^*) \\ &= Q(Ax + B(x)u + G) - Q\dot{x}_{\text{load}}^* \\ &= 0 \end{aligned} \tag{17}$$

When $u = u_{\text{eq}}$, this implies solving (17) gives a result which when solved part by part yields:

$$u_{\text{eq\_d}} = \frac{c_i\left(-\dfrac{R_{\text{fm}}}{L_{\text{fm}}}x_1 + \omega x_1 + \dfrac{v_d}{L_{\text{fm}}} - \dot{x}_1^*\right)}{c_i\dfrac{x_3}{L_{\text{fm}}} + c_v\dfrac{x_1}{c}} + \frac{c_v\dfrac{x_1}{c}\left(\omega x_1 + \dfrac{R_{\text{fm}}}{L_{\text{fm}}}x_2 + \dot{x}_2^*\right)}{\dfrac{x_3}{L_{\text{fm}}}\left(-c_i\dfrac{x_3}{L_{\text{fm}}} + c_v\dfrac{x_1}{c}\right)} \tag{18a}$$

$$u_{\text{eq\_q}} = -\frac{L_{\text{fm}}}{x_3}\left(\omega x_1 + \frac{R_{\text{fm}}}{L_{\text{fm}}}x_2 + \dot{x}_2^*\right) \tag{18b}$$

D. Stability Evaluation of SM Control

A more general method of Lyapunov theory is used for exploring the stability of system states in the time domain for both linear and nonlinear system. Assuming a Lyapunov function given below

$$V(s_s) = s_s^T H s_s \tag{19}$$

where s_s^T is the transpose of the column vector s_s. To render $V(s_s) > 0$, the matrix H must be positive definite (if and only if all its determinates are positive). Now, to obtain a sufficient condition for the stability in the sliding mode surface operation, given the form of Lyapunov function as in (19) Then, the Lyapunov function, in this case, is given as:

Hence, evaluating the second condition of the Lyapunov function, $\dot{V}(s_s) \le 0$ for all s_s, for the continuous system. We have that

$$\dot{V}(s_s) = \dot{s}_s^T s_s + s_s^T \dot{s}_s = f^T(s_s)s_s + s_s^T f(s_s) \qquad (20)$$

Thus, (19) must be less than zero for the existence of the sliding mode to ensure the trajectory attraction toward the switching surface. If it happens that the initial state vector $x(t_o)$ is not on the sliding surface (s_s) or that there is a deviation from the sliding surface due to nonlinear load parameter variations and disturbances. The control law must hence enforce the trajectory to reach the sliding surface and to stay on it. Applying the control law given by equations of switching part and using (20) with $u = u_{\text{eq}} + \text{sgn}(s_s)$, the time derivate of s_s becomes:

$$\begin{aligned}\dot{s}_{\text{si}} &= Q(Ax + B(x)(u_{\text{eq}} + \text{sgn}(s_s)) + G) - Q\dot{x}^* \\ &= QB(x)\,\text{sgn}(s_s)\end{aligned} \qquad (21)$$

Hence, the time derivate is given as $\dot{V}(s_s) = s_s^T \dot{s}_{\text{si}} < 0$ must hold when $s_s \ne 0$ Thus,

$$\dot{V}(s_s) = s_s^T QB(x)\,\text{sgn}(s_{\text{si}}) \qquad (22)$$

Which implies the sufficient condition for $\dot{V}$ to be a negative-definite function, simplified as

$$\dot{V}(s_s) = \left(-c_i x_3 + \frac{l_{\text{fm}}}{c_f} \left(\frac{x_1 \,\text{sgn}(s_{\text{sd}}) + x_2 \,\text{sgn}(s_{\text{sq}})}{s_{sd} \,\text{sgn}(s_{\text{sd}}) + s_{sq} \,\text{sgn}(s_{\text{sq}})} \right) (c_v s_{\text{sd}}) \right) \times \frac{s_{\text{sd}} \,\text{sgn}(s_{\text{sd}}) + s_{\text{sq}} \,\text{sgn}(s_{\text{sq}})}{l_{\text{fm}}} \qquad (23)$$

Thus, the stability criterion is

$$-c_i x_3 + \frac{l_{\text{fm}}}{c_f} \left(\frac{x_1 \,\text{sgn}(s_{\text{sd}}) + x_2 \,\text{sgn}(s_{\text{sq}})}{s_{\text{sd}} \,\text{sgn}(s_{\text{sd}}) + s_{sq} \,\text{sgn}(s_{\text{sq}})} \right) c_v s_{\text{sd}} < 0 \qquad (23a)$$

This implies that:

$$\begin{aligned}&-c_i x_3 + c_v \frac{l_{\text{fm}}}{c_f} \left(x_1 \frac{\text{sgn}(s_{\text{sq}}) s_{\text{sd}}}{\text{sgn}(s_{\text{sd}}) + \text{sgn}(s_{\text{sq}})} \right) + \\ &c_v \frac{l_{\text{fm}}}{c_f} \left(x_2 \frac{\text{sgn}(s_{\text{sq}}) s_{\text{sd}}}{\text{sgn}(s_{\text{sd}}) + \text{sgn}(s_{\text{sq}})} \right) < 0\end{aligned} \qquad (23b)$$

Thus, the sufficient condition for equation (23) to be verified is

$$\begin{aligned}&-c_i x_3 + c_v \frac{l_{\text{fm}}}{c_f} \left(|x_1| \frac{\text{sgn}(s_{\text{sq}}) s_{\text{sd}}}{|s_{\text{sd}}| + |s_{\text{sq}}|} \right) + \\ &c_v \frac{l_{\text{fm}}}{c_f} \left(|x_2| \frac{\text{sgn}(s_{\text{sq}}) s_{\text{sd}}}{|s_{\text{sd}}| + |s_{\text{sq}}|} \right) < 0\end{aligned} \qquad (23c)$$

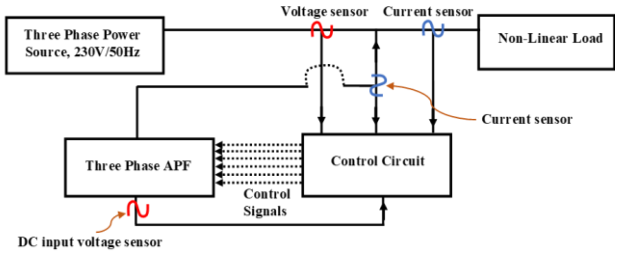

Fig. 3. Block diagram of the APF with the coupling filter

Assuming that

$$|x_1| \frac{\text{sgn}(s_{\text{sq}}) s_{\text{sd}}}{|s_{\text{sd}}| + |s_{\text{sq}}|} \le |x_1| \text{ and } |x_2| \frac{\text{sgn}(s_{\text{sq}}) s_{\text{sd}}}{|s_{\text{sd}}| + |s_{\text{sq}}|} \le |x_2|$$

Hence, for $\dot{V}(s_s) < 0$ we arrive the sufficient condition:

$$\frac{l_{\text{fm}}}{c_f} (c_v) \left(|x_1| + |x_2| \right) < c_i x_3 \qquad (24)$$

The inequality was satisfied by a careful selection of the sliding mode surface coefficients c_i and c_v to ensure speedy convergence of the state variables. From the knowledge of the nonlinear load ratings, assuming maximum possible values of the currents in the *d-q* model and maximum input voltage to the APF; putting these maximum values in (24), one can select the parameters c_i and c_v by trial and error method. Fig. 3 shows the block diagram of the complete system.

E. PQ Theory Algorithm

PQ theory algorithm is derived as shown in equations below. Given line to neutral voltage as u_{sa} , u_{sb} , and u_{sc} the transformed voltage is gotten as

$$\begin{bmatrix} u_{s\alpha} \\ u_{s\beta} \end{bmatrix} = \sqrt{\frac{2}{3}} \begin{bmatrix} 1 & -\frac{1}{2} & -\frac{1}{2} \\ 0 & \frac{\sqrt{3}}{2} & -\frac{\sqrt{3}}{2} \end{bmatrix} \begin{bmatrix} u_{\text{sa}} \\ u_{\text{sb}} \\ u_{\text{sc}} \end{bmatrix} \qquad (25)$$

Also, given the current on the lines as i_{sa}, i_{sb}, and i_{sc}, hence the transformed current is obtained using similar trend as in (25).

The instantaneous real and reactive power of the system denoted as p and q is stated as

$$\begin{bmatrix} p \\ q \end{bmatrix} = \begin{bmatrix} u_{s\alpha} & u_{s\beta} \\ u_{s\beta} & -u_{s\alpha} \end{bmatrix} \begin{bmatrix} i_{s\alpha} \\ i_{s\beta} \end{bmatrix} \qquad (26)$$

Now, to calculate α, β compensation current, it implies that

$$\begin{bmatrix} i_{c\alpha} \\ i_{c\beta} \end{bmatrix} = \frac{1}{u_\alpha^2 + u_\beta^2} \begin{bmatrix} u_{s\alpha} & u_{s\beta} \\ u_{s\beta} & -u_{s\alpha} \end{bmatrix} \begin{bmatrix} -p + p_{\text{loss}} \\ -q \end{bmatrix} \qquad (27)$$

III. Simulations, Results and Discussions

Simulations are carried-out for the system without APF control and with APF using both SM and PQ control algorithms. The system parameters are shown in Table I while a summary of control parameters for PQ and SM control algorithms are shown in Table II.

TABLE I: SYSTEM PARAMETERS

Parameters	Values
Phase-to-phase V_{rms} voltage source	295V
Frequency	50Hz
Base voltage V_{rms} (phase to phase)	295V
X/R	2
Load resistance and inductance	R_{load}=200Ω, L_{load}=10mH

TABLE II: SUMMARY OF CONTROL PARAMETERS FOR PQ AND SMC

Control parameters	Values	
	PQ	SMC
Butterworth low pass filter passband edge frequency	314.159 rad/sec	314.159 rad/sec
PI controller	$K_i = 2.654$ $K_p = 3.6$	--
Coefficient of the switching surface	--	$c_i = 0.8$ $c_v = 0.24$
Reference voltage	$V_{\mathrm{ref}} = 400$ V	$V_{\mathrm{ref}} = 400$ V
Coupling resistor and inductor	R =2 Ω L=4.5mH	R =2 Ω L=4.5mH

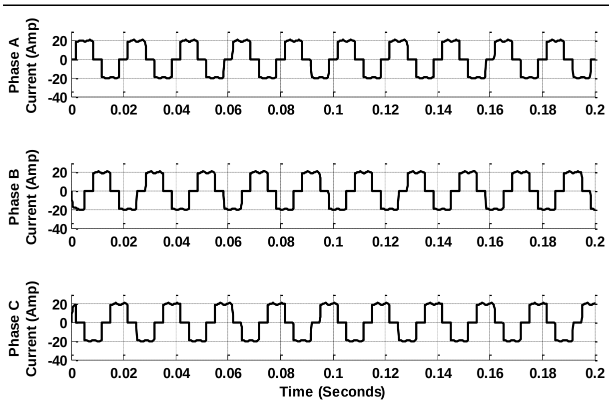

Fig. 4. Line current (A) without the APF at PCC

First, the grid is simulated without APF but with nonlinear load connected. The line current of the grid as shown in Fig. 4 is non-sinusoidal and continues all through the grid, interfering with other loads connected to the network. This is because of three-phase rectifiers connected to an R-L load. As a result, there is severe harmonics distortion, up to THD value of 29.97% per phase as in Fig. 5. This is because of the nonlinear load connected to the network. This effect needs to be mitigated for the safety of other loads in the grid, hence the need for APF. Thus, to protect other loads in the network from being affected by the harmonic generated, the source of the harmonics (load side) need to be shunted from entering the network and other loads in the grid. The APF is connected to shunt these effects by returning the non-sinusoidal load current to near sinusoidal.

Low pass filter was used as an optimal strategy to obtain improved steady state results while using no coupling transformer and no passive filter in coupling the APF. This helped to reduce cost of control implementation. The value of the filter was tuned to an optimal value to effectively filter-out noise and high-frequency harmonic components. Fig. 6 shows the line current when the SM controlled- APF was connected while Fig. 7 shows the harmonic content of the three phases.

Finally, PQ algorithm was used to control the APF to compare its behaviour with SMC techniques following the same timing sequence achieved earlier. The results obtained are as follows in Fig. 8. In addition, the % THD are shown in Fig. 9.

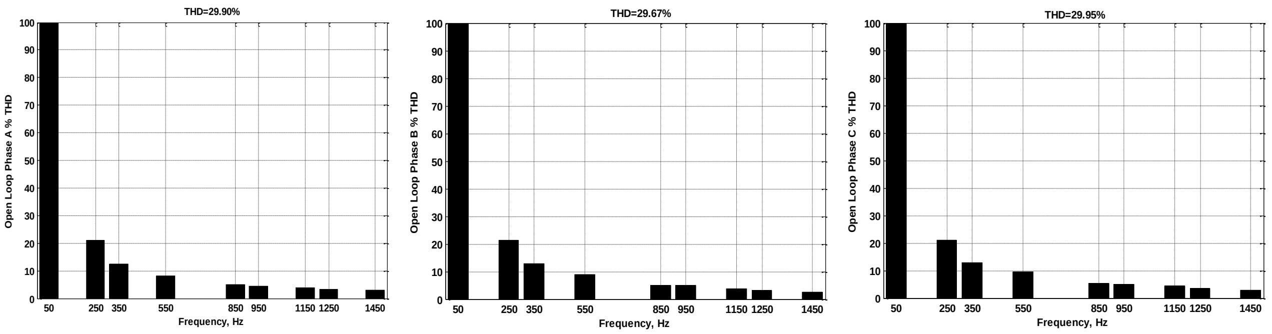

Fig. 5. % THD against frequency (Hz) without APF

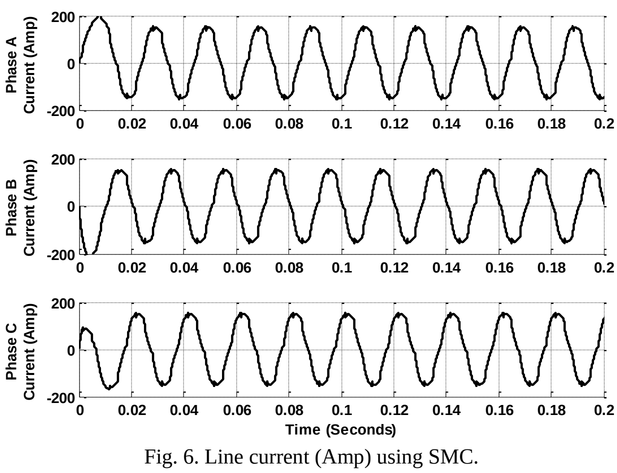

Fig. 6. Line current (Amp) using SMC.

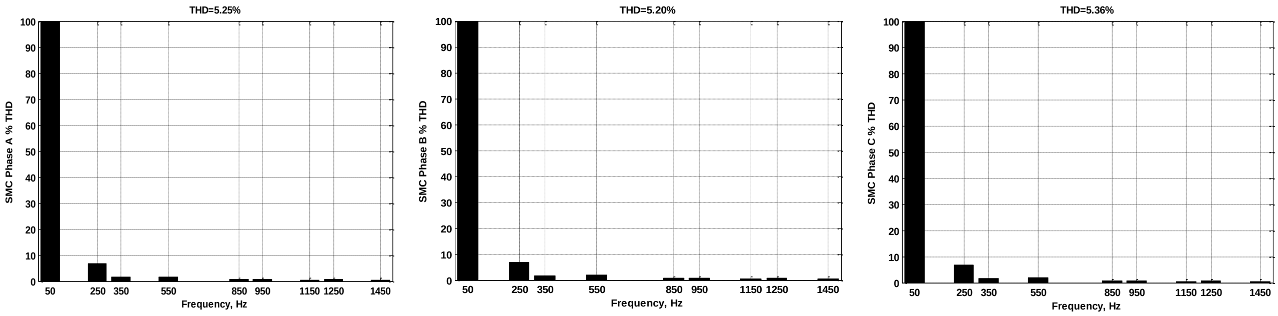

Fig. 7. % THD against frequency (Hz) with APF using SMC

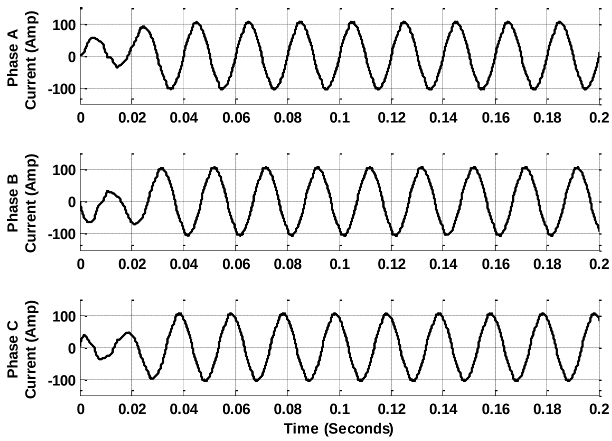

Fig. 8. Plot of line current (Amp) with PQ control method.

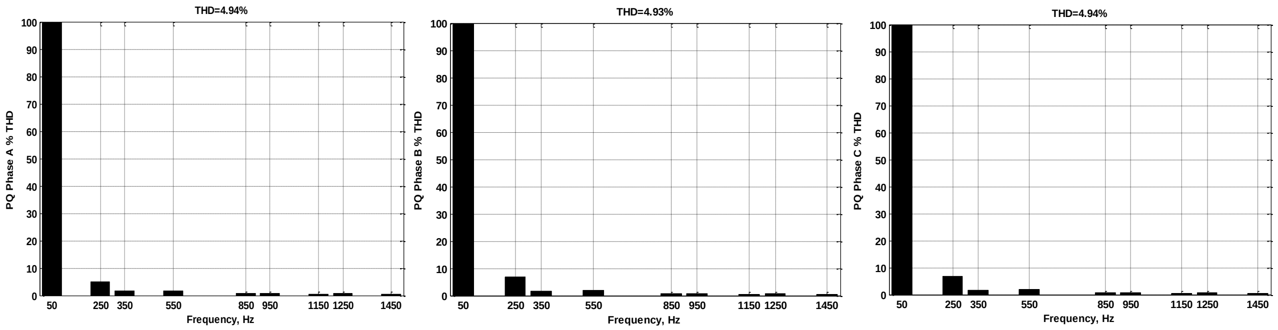

Fig. 9. % THD against frequency (Hz) with PQ control method

The results obtained show that when the APF is connected to the grid using either of the control methods, it shunts the harmonic from the nonlinear load from entering the grid. In both SM and PQ methods, the grid phase and line voltages remain undistorted.

Based on the analysis already made, it is clear that there are deviations as regards to the operation of the PQ Theory and SMC control techniques. The transformation algorithm for PQ is based on α-β transformation (AC) while the SMC is based on d-q reference frame (DC). This technically implies that there is a real and reactive power manipulation in PQ and none in SMC. In addition, due to the presence of PI controller in PQ and switching function in SMC for dc regulation, there is an improved THD (%) in PQ than in SMC although the response of SMC to transients is faster than in PQ.

However, in both techniques, a set of transformation, which reduces harmonics in the grid using Butterworth and Coupling Filters, were developed. A hysteresis carrier-less comparator was used in both techniques for circuit complexity reduction.

IV. Conclusion

The results obtained show that SM control and PQ theory control are good techniques for controlling APF to achieve harmonic mitigation in power grids. The results obtained show that PQ theory offered slightly better performance than the SM control even though the algorithm and steps for implementation of SM is simpler due to the use of programable chips. In addition, the execution time for implementation of the PQ theory control was more than that for the SM control. Thus, SM control remains more flexible to execute than the PQ control method. The PQ control theory reduced the THD value on average from 29.84% to 4.937% while the SM control reduced the THD value on average from 29.84% to 5.27%. However, both values were in conformity with the IEEE recommended standard for a system in the voltage level considered.

CONFLICT OF INTEREST

The authors declare no conflict of interest.

AUTHOR CONTRIBUTIONS

Eric Nwokolo developed the SM and PQ control algorithms for the shunt active power filter. Ifeanyi Chinaeke-Ogbuka and Augustine Ajibo provided research assistance in the modelling and simulation of the control algorithms in MATLAB/Simulink environment. Cosmas Ogbuka and Uche Ogbuefi wrote the final version of the paper and undertook the revisions throughout the editorial process. Cosmas Ogbuka, specifically, served as the corresponding author. Emenike Ejiogu is the Professor and Head of Lab. He initiated the research idea and secured the support of the Africa Centre of Excellence for Sustainable Power and Energy Development (ACE-SPED) where he also serves as the Director/Centre Leader.

ACKNOWLEDGMENT

The authors acknowledge the support received from the Africa Centre of Excellence for Sustainable Power and Energy Development (ACE-SPED), University of Nigeria, Nsukka that enabled the timely completion of this research.

REFERENCES

[1] J. Huang and Z. Jiang, “Power quality assessment of different load categories,” *Energy Procedia*, vol. 141, pp. 345-351, Dec. 2017.

[2] R. Sinvula, K. M. Abo-Al-Ez, and M. T. Kahn, “Harmonic source detection methods: A systematic literature review,” *IEEE Access*, vol. 7, pp. 74283-74299, Jun. 2019.

[3] C. M. Nwosu, C. U. Ogbuka, and S. E. Oti, “A comparative analysis of control strategies for low harmonic rectifier having DC to DC converter,” *R. Adv. Electr. Electron. Eng*., vol. 11, no. 4, pp. 1-11, 2018.

[4] C. U. Ogbuka and M. U. Agu, “A generalized rectified sinusoidal PWM technique for harmonic elimination,” *Pac. J. Sci. Technol*., vol. 10, no. 2, pp.21-26, 2009.

[5] S. N. S. Nasir, J. J. Jamian, and M. W. Mustafaet, “Minimizing harmonic distortion impact cause by CS using Meta heuristic technique," *Telkomnika*, vol. 17, pp.1992-2000, Aug. 2019.

[6] Z. Xin, P. Mattavelli, W. Yao, Y. Yang, F. Blaabjerg, and P. Chiang Loh, “Mitigation of grid-current distortion for LCL-filtered voltage-source inverter with inverter-current feedback control,” *IEEE Trans. Power Electron*., vol. 33, no. 7, pp. 6248-6261, 2018.

[7] S. Biricik, S. K. Khadem, S. Redif, and M. Basu M, “Voltage distortion mitigation in a distributed generation-integrated weak utility network via a self-tuning filter-based dynamic voltage restorer,” *Electr. Eng*., vol. 100, pp. 1857-1867, Nov. 2017.

[8] R. Rajagopal, K. Palanisamy, and S. Paramasivam, “Shunt active filter based on 7-level cascaded multilevel inverter for harmonic and reactive power compensation,” *J. Electr. Eng. Technol*., vol. 14, pp. 1543-1551, May 2019.

[9] H. Huang, L. Zhang, O. J. K. Oghorada, and M. Mao, “A delta-connected MMCC-based active power conditioner for unbalanced load compensation and harmonic elimination,” *Int. J. Electr. Power Energy Syst*., vol. 118, pp. 1-16, Jun. 2020.

[10] J. Turunen, M. Salo, and H. Tuusa, “Comparison of three series hybrid active power filter topologies,” in *Proc. IEEE 11th Int. Conf. on Harmonics and Quality of Power*, 2004, pp. 324-329.

[11] M. Haddad, S. Rahmani, A. Hamadi, A. Javadi, and K. Al-Haddad, “Harmonic mitigation using three level bidirectional neutral point clamped (BNPC) based three phase shunt active power filter,” in *Proc. IEEE Int. Conf. on Industrial Technology*, 2015, pp. 2526-2531.

[12] A. Zouidi, F. Fnaiech, and K. Al-Haddad, “Neural network controlled three phase three wire shunt active power filter,” in *Proc. IEEE Int. Symp. on Industrial Electronics*, Montreal, Que., Canada, July 2006, pp. 5-10.

[13] J. Xu, M. Chen, J. Ju, and D. Xu, “An improved harmonic detection based on lead compensation for active power filter,” in *Proc. IEEE 11th Workshop on Control and Modeling for Power Electronics*, Zurich, Switzerland, 2008, pp. 1-6.

[14] A. Luo, C. Tang, Z.K. Shuai, W. Zhao, F. Rong, and K. Zhou, “A novel three-phase hybrid active power filter with a series resonance circuit tuned at the fundamental frequency,” *IEEE Trans. Ind. Electron*., vol. 56, no. 7, pp. 2431-2440, Jul. 2009.

[15] A. Dell'Aquila, A. Lecci, and M. Liserre, “Microcontroller based fuzzy logic active filter for selective harmonic compensation,” in *Proc. IEEE Industry Applications Conf. 38th IAS Annual Meeting*, Salt Lake City, UT, USA, 2003, pp. 285-292.

[16] S. C. Ferreira, R. B. Gonzatti, R. R. Pereira, C. H. da Silva, L. E. B. da Silva, and G. Lambert-Torres, “Finite control set model predictive control for dynamic reactive power compensation with hybrid active power filters,” *IEEE Trans. Ind. Electron*., vol. 65, no. 3, pp. 2608-2617, 2018.

[17] L. Wang, C. Lam, and M. Wong, “Unbalanced control strategy for a thyristor-controlled LC-coupling hybrid active power filter in three-phase three-wire systems,” *IEEE Trans. Power Electron*., vol. 32, no. 2, pp. 1056-1069, 2017.

[18] H. Azeem, S. Yellasiri, V. Jammala, B. S. Naik, and A. K. Panda, “A fuzzy logic-based switching methodology for a cascaded H-bridge multi-level inverter,” *IEEE Trans. Power Electron*., vol. 34, no. 10, pp. 9360-9364, 2019.

[19] D. Suresh and S.P. Singh, “Type-2 fuzzy logic controlled three-level shunt active power filter for power quality improvement,” *Electr Pow Compo Sys*., vol. 44, no. 8, pp. 873-882, 2016.

[20] K. Haghdar and H. A. Shayanfar, “Selective harmonic elimination with optimal DC sources in multilevel inverters using generalized pattern search,” *IEEE Trans on Industrial Informatics*, vol. 14, no. 7, pp. 3124-3131, 2018.

[21] M. Sharifzadeh, H. Vahedi, R. Portillo, L.G. Franquelo, and K. Al-Haddad, “Selective harmonic mitigation based self-elimination of triplen harmonics for single-phase five-level inverters,” *IEEE Trans. Power Electron*., vol. 34, no. 1, pp. 86-96, 2019.

[22] M. Badoni, A. Singh, and B. Singh, “Comparative performance of wiener filter and adaptive least mean square-based control for power quality,” *IEEE Trans. Ind. Electron*., vol. 63, no. 5, pp. 3028-3037, 2016.

[23] R. Guzman, L. Garcia de Vicuna, J. Morales, M. Castilla, and J. Miret, “Model based control for a three-phase shunt active power filter,” *IEEE Trans. Ind. Electron*., vol. 63, no. 7, pp. 3998-4007, 2016.

[24] S. Rahmani, A. Hamadi, N. Mendalek, and K. Al-Haddad, “A new control technique for three-phase shunt hybrid power filter,” *IEEE Trans. Ind. Electron*., vol. 56, no. 8, pp. 2904-2915, 2009.

[25] T. Kamel, D. Abdelkader, B. Said, S. Padmanaban, and A. Iqbal, “Extended kalman filter-based sliding mode control of parallel-connected two five-phase PMSM drive system,” *Electronics*, vol. 7, no. 14, pp. 1-19, 2018

[26] P. Kanjiya, V. Khadkikar, and H. H. Zeineldin, “Optimal control of shunt active power filter to meet IEEE std. 519 current harmonic constraints under non-ideal supply condition,” *IEEE Trans. Ind. Electron.*, vol. 62, no. 2, pp. 724-734, 2015.

[27] B. R. Lin and C. H Huang, “Implementation of a three-phase capacitor-clamped active power filter under unbalanced condition,” *IEEE Trans. Ind. Electron*., vol. 53, no. 5, pp. 1621-1630, 2006.

[28] F. Briz, P. Garcia, M. W. Degner, D. D. Reigosa, and J. M. Guerrero, “Dynamic behaviour of current controllers for selective

harmonics compensation in three phase active power filters," *IEEE Trans. Ind. Appl*., vol. 49, no. 3, pp. 1411-1420, 2013.

[29] D. Raveendhra and M. K. Pathak, "Three-phase capacitor clamped boost inverter," *IEEE Trans. Emerg. Sel. Topics Power Electron*, vol. 7, no. 3, pp. 1999-2011, 2019.

[30] Y. B. Chiu, G. W. Chang, Y. Y. Chen, L. Y. Hsu, H. J. Lu, Y. D. Lee, and Y. R. Chang, "Neural network-based approach for determining optimal reference compensation current of shunt active power filter," presented at IEEE Power and Energy Society General Meeting (PESGM 2016), Boston Ma. 17-21 July 2016.

[31] J. Morales, L. Vicuña, R. Guzman, M. Castilla, and J. Miret, "Modeling and sliding mode control for three-phase active power filters using the vector operation technique," *IEEE Trans. Ind. Electron.*, vol. 65, no. 9, pp. 6828–6838, 2018.

[32] Y. Chen and J. Fei, "Dynamic sliding mode control of active power filter with integral switching gain," *IEEE Access*, vol. 7, pp. 21635–21644, Feb. 2019.

[33] J. Fei and Y. Chu, "Double hidden layer output feedback neural adaptive global sliding mode control of active power filter," *IEEE Trans. Power Electron*., vol. 35, no. 3, pp. 3069-3084, 2020.

Eric Nwokolo graduated from the Department of Electrical Engineering, University of Nigeria Nsukka, in 2013 and 2019 where he obtained his B.Eng. degree (Second Class Upper division) and M.Eng. degree (Distinction) respectively. His research interests include Power Electronics, Power System, and Renewable Energy. Ahead of his doctoral research, he is currently collaborating in research at the Department of Electrical Engineering, University of Nigeria, Nsukka.

Ifeanyi Chinaeke-ogbuka was born in Nsukka Nigeria on 14th September 1989. She obtained her Bachelor degree of Engineering in electronic engineering and Master degree of Engineering also in Electronic Engineering Department of the University of Nigeria, Nsukka. She currently serves as a Lecturer II in the same Department. Her research interests are in Electronic, Communications, Control, and Instrumentation. She is a member of the Nigerian Institution of Electrical and Electronic Engineers (NIEEE). She has published in peer-reviewed journals and presented papers in refereed conferences.

Augustine Ajibo is an academic staff of the Department of Electronic Engineering, University of Nigeria Nsuuka, Enugu-Nigeria. He obtained his B.Eng. and M.Eng. degrees in Electronic Engineering and Telecommunication Engineering respectively from the same department. He is currently undergoing his Ph.D. studies at the Department of Systems Innovation, Graduate School of Engineering Science, Osaka University, Japan. He has over the years published research articles in reputable journals and conferences. His research interest includes Artificial Intelligence, Natural Language Processing, Human-Robot-Interaction, and Cognitive Science, Internet of Things (IoT), Cloud computing, Big Data, Wireless networks.

Cosmas Ogbuka holds the following degrees from the Department of Electrical Engineering, University of Nigeria Nsukka, where he has attained the rank of Senior Lecturer: B.Eng. (First Class Honors), M.Eng. (Distinction) and Doctor of Philosophy (Ph.D.) obtained in 2004, 2009, and 2014 respectively. His research interests include Electrical Machines, Drives and Power Electronics. He is an International Faculty Fellow of the Massachusetts Institute of Technology (MIT) USA and had also undertaken a postdoctoral research visit at the Chair of Electrical Drives and Actuators (EAA) Universitaet der Bundeswehr Muenchen Germany. He is currently the Director of the Computer Communications Centre of the University of Nigeria, Nsukka

Uche Ogbuefi obtained her Doctorate Degree from the Department of Electrical Engineering, University of Nigeria, Nsukka in 2013 after having obtained a Post Graduate Diploma in Electrical Engineering in 2001 from Rivers State University of Science and Technology and a B.Eng. Degree from the Electrical/Electronic Engineering Department, University of Port Harcourt in 2009. Professional Qualifications: - Member, Nigeria Society of Engineer (.NSE) - COREN Registered - Member, Association of Professional Women in Engineering in Nigeria (APWEN), NSE Aba Branch Chairman's merit Award –2009. Her quest for academics is evident in her research work.

Emenike Ejiogu is a Professor of Power Electronics in the Department of Electrical Engineering, University of Nigeria Nsukka. He obtained his Doctor of Philosophy in Power Devices & Systems at Shinshu University, Nagano-city, Japan in 1994 and has been a Research Professor at Mirai Research Labaratory, High Tech Research Centre, Ritsumeikan University, Kustatsu-shi, Shiga-ken, Japan since 2009. He was the Director-General/Chief Executive Officer (CEO), MicroSilitron Inc., Laboratory, Biwako Campus, Faculty of Science & Engineering, Ritsumeikan University, Kusatsu-city, Japan from 2007 to 2009. He is the Principal Investigator of the Laboratory of Industrial Electronics, Power Devices and New Energy Systems, University of Nigeria Nsukka. He is also the Director/Centre Leader of the World Bank Africa Centre of Excellence for Sustainable Power and Energy Development (ACESPED), University of Nigeria, Nsukka. Prof. Ejiogu has over six (6) international patents/inventions in engineering to his credit and over 65 publications in peer reviewed international journals & conferences